

Original Article

Quantum dual-branch neural networks with transfer learning for early detection of skin cancer

Yuyang Sun, Xing Deng, Haijian Shao

School of Computer, Jiangsu University of Science and Technology, Zhenjiang 212100, Jiangsu, China

Received November 26, 2024; Accepted April 14, 2025; Epub May 15, 2025; Published May 30, 2025

Abstract: Background: Accurate classification of skin cancer is critical for early detection and timely treatment, significantly improving patient survival rates. While quantum neural networks combined with transfer learning show promise in medical image analysis, quantum noise remains a major challenge, compromising the stability and reliability of these systems. This study aims to address this limitation by developing a robust quantum-based framework for skin cancer classification. Methods: We propose a Quantum Dual-Branch Neural Network (QDBNN) that employs two independently trained network branches without shared weights. Dual-modal features are fused at the fully connected layer, and a Variational Quantum Classifier (VQC) is utilized for final classification. The model is evaluated on two datasets: the multiclass HAM10000 and the binary Malignant vs. Benign dataset. Results: QDBNN achieved state-of-the-art accuracies of 93.6% on HAM10000 and 93.5% on the Malignant vs. Benign dataset, outperforming classical and quantum transfer learning baselines. The dual-branch architecture and weighted feature fusion demonstrated enhanced robustness against quantum noise while improving generalization. Conclusion: QDBNN effectively mitigates quantum noise interference and leverages quantum-classical hybrid advantages for skin cancer classification. Its success highlights the potential of quantum-inspired architectures in medical imaging, offering a pathway toward clinically deployable tools for early diagnosis. Future work will focus on hardware optimization and scalability to larger datasets.

Keywords: Quantum computing, skin cancer diagnosis, deep learning

Introduction

Medical image classification represents a critical yet challenging research domain, necessitating precise analysis and interpretation of complex, high-dimensional medical imaging data [1]. This task's fundamental challenges stem from the inherent diversity and complexity of medical images, encompassing morphological variations in lesions, poor contrast between pathological and healthy tissues, and acquisition-related noise and artifacts [2, 3]. Additionally, individual patient differences can lead to considerable variability in lesion appearances, further complicating the accuracy and reliability of classification.

Within the spectrum of medical image classification applications, automated skin cancer classification emerges as a paramount concern. Skin cancer is one of the most prevalent

cancers worldwide, with melanoma and non-melanoma skin cancers being the two main categories. Despite its lower incidence, melanoma exhibits high malignancy and rapid progression characteristics [4]. Once melanoma reaches an advanced stage, the effectiveness of treatment diminishes considerably, highlighting the critical importance of early detection and intervention in improving patient survival. Conventional skin cancer diagnosis predominantly depends on dermatologists' expertise and subjective assessment, subject to variables including clinical experience and cognitive fatigue. The advent of automated classification systems offers a more efficient and objective diagnostic method, significantly enhancing early detection accuracy while minimizing the risks of misdiagnosis and missed diagnoses [5]. These technologies not only improve diagnostic efficiency but also provide more reliable health protection for both doctors and patients.

Classical neural networks, despite their proven effectiveness, demand intensive computational resources, especially when processing high-dimensional and heterogeneous medical imaging data [6]. Quantum neural networks, however, offer a promising solution to these challenges due to their inherent parallel computing capabilities. In 2003, Anguita [7] pioneered the application of quantum computing in training support vector machines (SVM), specifically addressing scenarios where classical quadratic programming methods proved inadequate. Their findings demonstrated that quantum computing provides significant parallel processing advantages over traditional optimization techniques in large-scale digital implementations, highlighting its potential to solve complex problems. The rapid evolution of quantum computing has established quantum neural networks as an innovative computational paradigm, positioning them at the forefront of contemporary research. Cong [8] introduced Quantum Convolutional Neural Networks (QCNN) in 2019, demonstrating efficient data encoding for N-qubit systems using only $O(\log(N))$ variational parameters. In 2023, Zhiguo Qu [9] introduced an intelligent diagnostic multimodal fusion system based on quantum neural networks, integrating QCNN features with other modalities to train effective variational quantum classifiers (VQC) for intelligent diagnosis. This system achieved notable success in diagnosing breast cancer and COVID-19. Additionally, in 2023, Juhyeon Kim [10] integrated QCNN with transfer learning techniques, employing various QCNN models to classify the MNIST dataset through quantum convolution and pooling operations. Their results demonstrated that quantum transfer learning outperformed traditional classical transfer learning models.

Despite the substantial potential of quantum neural networks, multiple fundamental challenges persist in their implementation and optimization. The vanishing gradient phenomenon remains a critical impediment to quantum deep learning advancement, necessitating innovative solutions that account for the distinct characteristics of quantum computing systems. Additionally, the limitations of current quantum devices present further obstacles for the practical implementation of quantum neural networks, demanding the development of algo-

rithms specifically tailored to these devices. Achieving quantum advantage is still a critical issue, particularly in terms of designing algorithms that can demonstrate the superiority of quantum computing in specific scenarios. To address these challenges, we propose a novel quantum neural network architecture for skin cancer segmentation: the Quantum Dual-Branch Neural Network (QDBNN), which combines quantum convolutional neural networks, transfer learning, and feature fusion techniques.

In recent years, research on skin lesion classification based on deep learning has made significant progress. Researchers have proposed a variety of innovative methods focusing on model architecture optimization, feature fusion, interpretability enhancement, and addressing data imbalance issues.

In terms of model architecture design, Gajera [11] conducted a comprehensive analysis of eight pre-trained CNN models and found that DenseNet-121 combined with a multilayer perceptron (MLP) performed best in multiple benchmark tests, achieving an accuracy of 81% on the HAM10000 dataset. The performance advantage of this combination stems from the dense connectivity structure's effective extraction of fine-grained features of skin lesions. Kumar [12] took a different approach by proposing to fuse handcrafted features from the image domain, spectral domain, and cepstral domain, and designed a one-dimensional multi-head CNN for classification. The accuracy on the HAM10000 dataset was improved to 89.71%, verifying the supplementary role of hybrid domain features for lesion spectral information.

Addressing the issues of model interpretability and decision credibility, Dakhli and Barhoumi [13] proposed an ensemble framework based on Dempster-Shafer evidence fusion. Through statistical tests and XAI feature visualization analysis of model failure cases, they selected models with strong complementarity for evidence fusion. The final accuracy was increased by 6% compared to a single model, reaching 92%. Similarly, Nguyen [14] introduced a soft attention mechanism to automatically locate lesion heatmaps and combined it with metadata such as age and gender. They achieved an

accuracy of 90% on InceptionResNetV2. The novel loss function they proposed alleviated the data imbalance problem, improving the F1-score to 0.81. Hasan [15] compared CNN models for skin cancer detection on Skin Cancer: Malignant vs. Benign datasets, achieving 93.18% accuracy with VGG16, while Huang [16] proposed Deep-skin integrating attention mechanisms and ensemble learning, attaining 87.8% accuracy on similar tasks.

Lightweight model design has become a focus for mobile medical applications. Hoang [17] developed a lightweight framework based on entropy-weighted segmentation (EW-FCM) and Wide-ShuffleNet. The number of parameters was reduced by 11 times compared to traditional models, while still maintaining an accuracy of 86% on the HAM10000 dataset, and the inference speed was increased by 30 times. The Tajerian [18] team used EfficientNet-B1 to build a web-based diagnostic tool, achieving a classification accuracy of 84.3% through data augmentation and transfer learning, providing feasibility validation for clinical deployment.

Traditional machine learning methods often rely on classical feature extraction techniques, which encounter challenges in medical imaging due to limited dataset sizes and resource-intensive processing requirements. These limitations become especially pronounced when capturing fine pathological features, such as subtle texture variations in skin cancer images, which necessitate more advanced methods. To overcome these challenges, our study proposes an innovative quantum-based approach.

Materials and methods

Dataset

The performance evaluation of the QDBNN architecture was conducted using two benchmark datasets: HAM10000 [19] and Skin Cancer: Malignant vs. Benign. The HAM10000 dataset, illustrated in **Figure 1**, comprises seven distinct classes of skin cancer lesions, specifically curated for pigmented skin lesions. The dataset encompasses 10,015 high-resolution dermoscopic images, capturing comprehensive dermatological features including texture patterns, color variations, and morphological characteristics. Each image is annotated by derma-

tology experts, providing high-quality labels for lesion types. The HAM10000 dataset exhibits notable class imbalance, with the “Melanocytic nevi” category comprising 6,705 images (67% of the total dataset). This imbalance presents challenges for the model’s generalization ability and increases the risk of overfitting.

The Skin Cancer: Malignant vs. Benign dataset facilitates binary classification of dermatological lesions, distinguishing between benign and malignant manifestations. It contains 3297 RGB images with a resolution of 224×224, of which 1,800 are benign and 1,497 are malignant. This dataset provides a solid platform for evaluating the performance of the QDBNN architecture in skin cancer detection.

Quantum convolutional neural networks

Convolutional Neural Networks (CNNs) have emerged as a paramount architecture in machine learning, demonstrating exceptional efficacy in classification tasks, particularly in image recognition domains. In recent years, CNNs have made significant strides in image recognition, object detection, image generation, and various other fields, becoming a cornerstone of computer vision and deep learning research. The Quantum Convolutional Neural Network (QCNN) is a machine learning model that integrates quantum computing with convolutional neural networks. Through the exploitation of quantum mechanical phenomena, specifically superposition and entanglement, QCNN achieve enhanced computational efficiency and accelerated processing capabilities.

In quantum convolutional neural networks, information is represented by quantum bits, which can be in superposition at the same time, that is, their quantum states can be represented as a linear combination of states $|0\rangle$ and $|1\rangle$. This means that the state of a single quantum bit can be described in quantum mechanics as, where $\alpha|0\rangle + \beta|1\rangle = 1$, α and β are complex coefficients. This means that a quantum bit can exist in multiple possible states at the same time until it is measured. $|\psi\rangle$ is the initial quantum state of the quantum system and M_m is the measurement operator, and the probability measurement formula is given by Eq. (1).

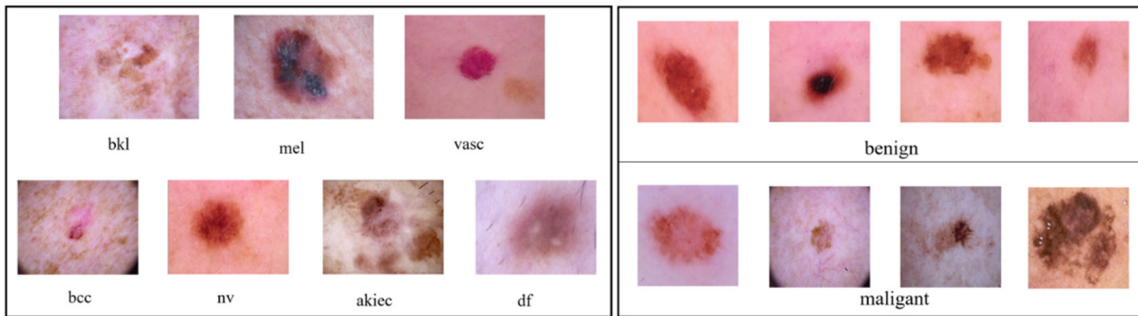


Figure 1. HAM10000 dataset and Malignant vs. Benign dataset.

Operator	Pauli-X	Hadamard	RY	Controlled Not	Controlled Z	RY Cnot
Gate						
formula	$\begin{bmatrix} 0 & 1 \\ 1 & 0 \end{bmatrix}$	$\frac{1}{\sqrt{2}} \begin{bmatrix} 1 & 1 \\ 1 & -1 \end{bmatrix}$	$\begin{bmatrix} \cos(\frac{\theta}{2}) & -\sin(\frac{\theta}{2}) \\ \sin(\frac{\theta}{2}) & \cos(\frac{\theta}{2}) \end{bmatrix}$	$\begin{bmatrix} 1 & 0 & 0 & 0 \\ 0 & 1 & 0 & 0 \\ 0 & 0 & 0 & 1 \\ 0 & 0 & 1 & 0 \end{bmatrix}$	$\begin{bmatrix} 1 & 0 & 0 & 0 \\ 0 & 1 & 0 & 0 \\ 0 & 0 & 1 & 0 \\ 0 & 0 & 0 & -1 \end{bmatrix}$	$\begin{bmatrix} 1 & 0 & 0 & 0 \\ 0 & 1 & 0 & 0 \\ 0 & 0 & \cos(\frac{\theta}{2}) & -\sin(\frac{\theta}{2}) \\ 0 & 0 & \sin(\frac{\theta}{2}) & \cos(\frac{\theta}{2}) \end{bmatrix}$

Figure 2. Diagram of a basic quantum gate and its formula.

$$p(m) = \langle \psi | M_m^\dagger M_m | \psi \rangle$$

In contrast to classical convolutional networks' numerical operations, quantum convolution implements unitary transformations on the quantum state vector, preserving quantum mechanical properties. The transformation methodology is determined by the characteristics of the quantum gates comprising the unitary operation. **Figure 2** illustrates the fundamental quantum gate operations. The Pauli-X gate flips the quantum bit from $|0\rangle$ to $|1\rangle$, the Hadamard gate [20] creates a superposition state for the quantum system, and the RY gate rotates the quantum bit by a specific numerical phase. Such rotation gates can be utilized for both feature encoding and parameter encoding in Quantum Convolutional Neural Networks (QCNNs).

The QCNN's quantum layer transforms classical data into quantum states through various encoding schemes, including angle encoding

[21] and amplitude encoding. When the quantum system is initialized, the eigenstate $|0\rangle$ is converted into a superposition state $(|0\rangle + |1\rangle)/\sqrt{2}$ through the action of the Hadamard gate. Subsequently, the phase is shifted and rotated through the unitary gate containing the encoded data.

A controlled quantum gate operation is implemented to establish entanglement correlations between qubits within the quantum system. Quantum entanglement is a critical resource in quantum computing, enabling the formation of non-classical correlations between quantum bits. The quantum measurement protocol extracts state information and maps expectation values to corresponding output channels, enabling classical information retrieval. Quantum measurement represents the final step in quantum information processing, where quantum information is converted into classical information, allowing it to be further processed or interpreted.

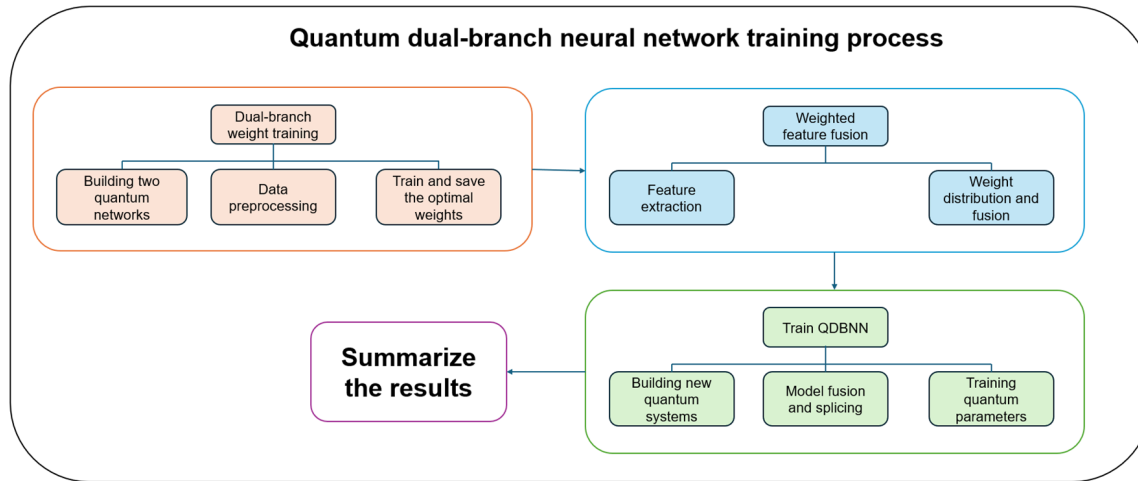


Figure 3. QDBNN train process.

QDBNN architecture

The quantum transfer learning method has shown promising results in classification tasks, such as breast cancer classification and gender prediction. Building on this, we propose the Quantum Dual-Branch Neural Network (QDBNN) architecture. The QDBNN architecture synergistically integrates quantum computing capabilities, transfer learning principles, and multi-model fusion strategies, yielding enhanced performance in dermatological malignancy classification. The training protocol, illustrated in **Figure 3**, encompasses three primary phases.

Dual-branch weight training

The initial phase comprises concurrent weight optimization of both network branches. Branch weight optimization is achieved through quantum transfer learning protocols. AlexNet [22] and VGG16 [23] have both played pivotal roles in advancing deep learning for image recognition. The implementation of deeper architectural paradigms has substantially augmented feature extraction capabilities. Through the utilization of compact convolutional and pooling kernels, these networks have improved the model's sensitivity to image features. These design principles have provided valuable insights and a solid foundation for the development of subsequent deep learning models. Based on this, the quantum pre-trained versions of AlexNet and VGG16 are selected as the dual branches of our network.

Custom-designed quantum neural networks were constructed to replace the fully connected layers within the pre-trained AlexNet and VGG16 architectures. The implemented quantum networks subsequently performed the classification tasks, replacing their classical counterparts, thereby enhancing the model's compatibility with the integrated QDBNN architecture and optimizing both data adaptability and model fitting performance. The skin cancer dataset was processed through the quantum-enhanced pre-trained models of AlexNet and VGG16, with optimal weights being automatically preserved after 100 training epochs.

Figure 4 illustrates the architectural design of the variational quantum classifier implemented in quantum transfer learning. After the intrinsic passes through the H gate, the quantum superposition state is constructed. Then the RY rotation gate is used to encode the features, and the RZ rotation gate is used to encode the trainable parameters and measure them after fitting. The formula is shown as in Eq. (2).

$$|\psi\rangle = \left(\bigotimes_{j=1}^m CY(\theta_j, q_{m-j}) \right) \cdot \left(\bigotimes_{i=1}^n RY(\theta_i, q_{n-i}) \right) \cdot (H^{\otimes n}) \cdot |0\rangle^{\otimes n}$$

Where n denotes the number of bits in the quantum network, RY(θ , q) denotes a rotation gate around the y-axis, where θ is the rotation angle and q is the quantum bit in action. CY(θ , q) represents a controlled y-revolving gate, where θ is the rotation angle and q is the quantum bit in action. Due to the fundamental differences between quantum neural networks and

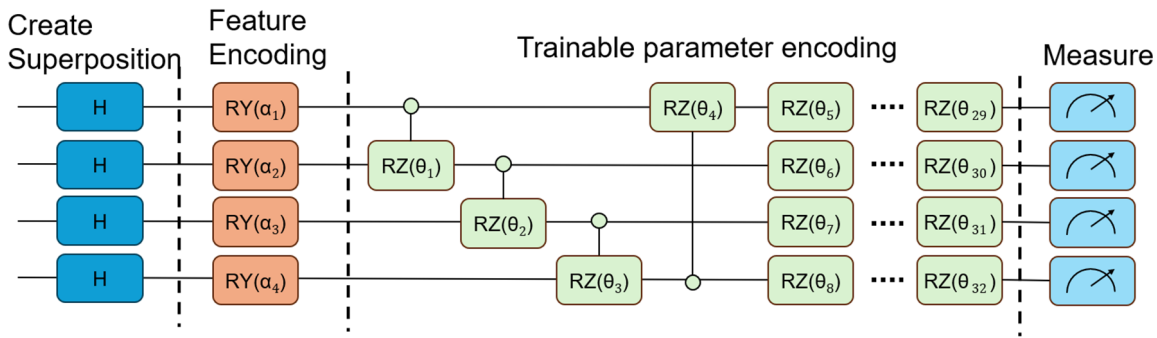


Figure 4. Variational quantum classifier in quantum transfer learning.

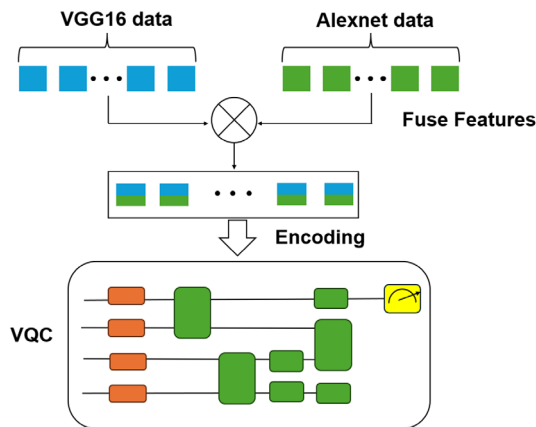


Figure 5. Feature fusion.

classical convolutional networks, traditional gradient computation methods are inapplicable. Consequently, the Parameter Shift Rule [24] is essential for gradient calculation in quantum neural networks. The Parameter Shift Rule is as follows:

The parameterized quantum gate in the gradient calculation process utilizing the Parameter Shift Rule is expressed as Eq. (3).

$$U_G(\theta) = e^{-ia\theta G} = I \cos(r\theta) - i \frac{a}{r} G \sin(r\theta)$$

Where $U(\theta)$ is the unitary operator and G is the Hermitian operator of the gate, which determines the nature of the quantum evolution. The objective function is Eq. (4).

$$f(\theta_1, \dots, \theta_n) = \langle \psi | U_G^\dagger(\theta_1) \cdots U_G^\dagger(\theta_n) A U_G(\theta_1) \cdots U_G(\theta_n) | \psi \rangle$$

When G has only two unique eigenvalues e_0 and e_1 , the derivative of the Parameter Shift Rule with respect to the parameters is Eq. (5).

$$\begin{aligned} \frac{\partial}{\partial \theta_i} &= f(\theta_1, \theta_2, \dots, \theta_n) \\ &= \langle \psi | [+ iaG] U_G^\dagger(\theta_i) A U_G(\theta_i) | \psi \rangle \\ &+ \langle \psi | [- iaG] U_G^\dagger(\theta_i) A U_G(\theta_i) | \psi \rangle \\ &= r \langle \psi | U_G^\dagger\left(\theta_i + \frac{\pi}{4}\right) A U_G\left(\theta_i + \frac{\pi}{4}\right) | \psi \rangle \\ &- r \langle \psi | U_G^\dagger\left(\theta_i - \frac{\pi}{4}\right) A U_G\left(\theta_i - \frac{\pi}{4}\right) | \psi \rangle \\ &= r [f\left(\theta_1, \dots, \theta_i + \frac{\pi}{4r}, \dots, \theta_n\right) - f\left(\theta_1, \dots, \theta_i - \frac{\pi}{4r}, \dots, \theta_n\right)] \end{aligned}$$

Where r is the shift constant, $r = \alpha/2 (e_1 - e_0)$. Following gradient computation via the Parameter Shift Rule, parameter updates are performed using the Adam optimization algorithm.

Weighted feature fusion

Weighted feature fusion enhances feature representation in deep learning models through differential weight assignment to diverse features, facilitating optimal information integration [25]. This methodology recognizes the heterogeneous contributions of multi-source and multi-type data to the target objective. The adaptive learning capability of weighted feature fusion enables optimal input balancing, thereby maximizing model performance. Based on its demonstrated efficacy, we integrated this mechanism into our framework.

As illustrated in **Figure 5**, the fully connected layers within the quantum pre-trained AlexNet and VGG16 models execute weighted feature fusion by assigning and combining weights to the processed network data. This methodology facilitates comprehensive information extraction while mitigating over-dependence on individual networks.

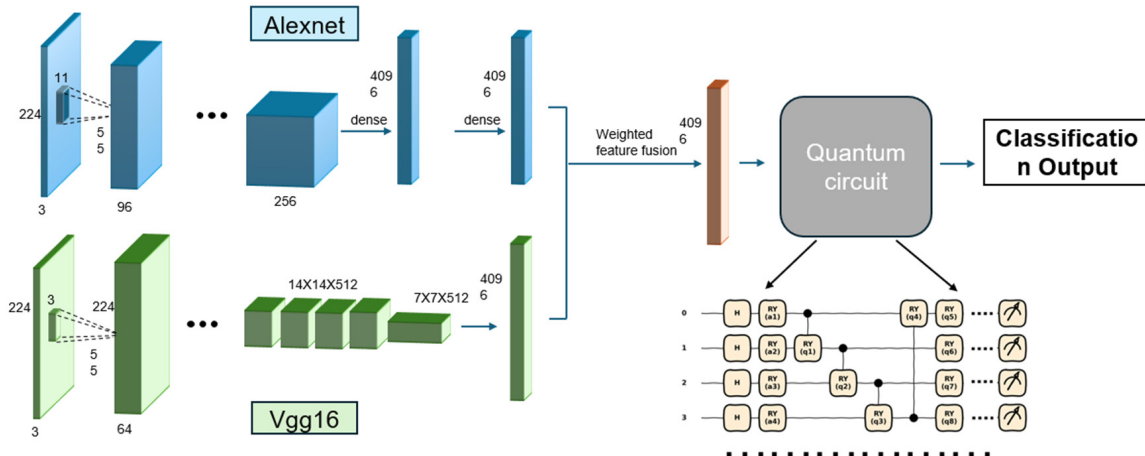


Figure 6. QDBNN.

During feature fusion optimization, a weighting function is implemented to systematically evaluate dual-branch feature contributions, ensuring optimal data utilization. We introduced accuracy-dependent weight coefficients to effectively allocate weights between VGG16 and AlexNet networks, ensuring multi-objective optimization outcomes. The objective function for the weighted solution is defined as Eq. (6).

$$W = \alpha W_1 + \beta W_2$$

W_1 and W_2 denote the features learned by the VGG16 and AlexNet networks, respectively. α and β represent the test accuracies of the two networks, with their squares serving as the weights for the networks. To reduce bias and improve stability in the solution, we introduce weight coefficients, ensuring that the solution is more balanced and robust.

Quantum two-branch network training

Following the previous step, we optimized the quantum pre-trained AlexNet and VGG16 models to obtain optimal weight parameters and subsequently performed weighted feature fusion. Next, we loaded these weights into the model and locked them in place. Subsequently, we implemented a dedicated quantum neural network with configured quantum gates for data encoding and established trainable quantum parameters to process the fused features. The training procedure specifically targeted the quantum parameters within the newly implemented network, facilitating the collapse of weight superposition states into corresponding

quantum state. This enabled nonlinear fitting and mapping of the data features, ultimately yielding the final results. The process is illustrated in **Figure 6**.

Figure 6 shows the overall architecture of the QDBNN model, which covers the entire experimental process. The data is trained and fitted through the dual branches of the network and finally encoded into the quantum system for further training and measurement.

Results

We present the classification results on two different skin cancer datasets. The implementation of a Quantum Convolutional Neural Network necessitates a quantum programming framework supporting quantum circuit operations, coupled with comprehensive tools for classical data preprocessing, training, and evaluation. The experimental implementation utilized PennyLane for quantum algorithm deployment and PyTorch for neural network training and data processing. The model was trained using sparse categorical cross-entropy as the loss function and optimized via the Adam optimizer.

Beyond accuracy metrics, we incorporated the Weighted-average F1 Score as a complementary performance indicator, computing individual F1 scores for each category and deriving their weighted average based on category-specific sample distributions. This method gives more weight to categories with more samples. The formula is Eq. (7).

Early detection of skin cancer

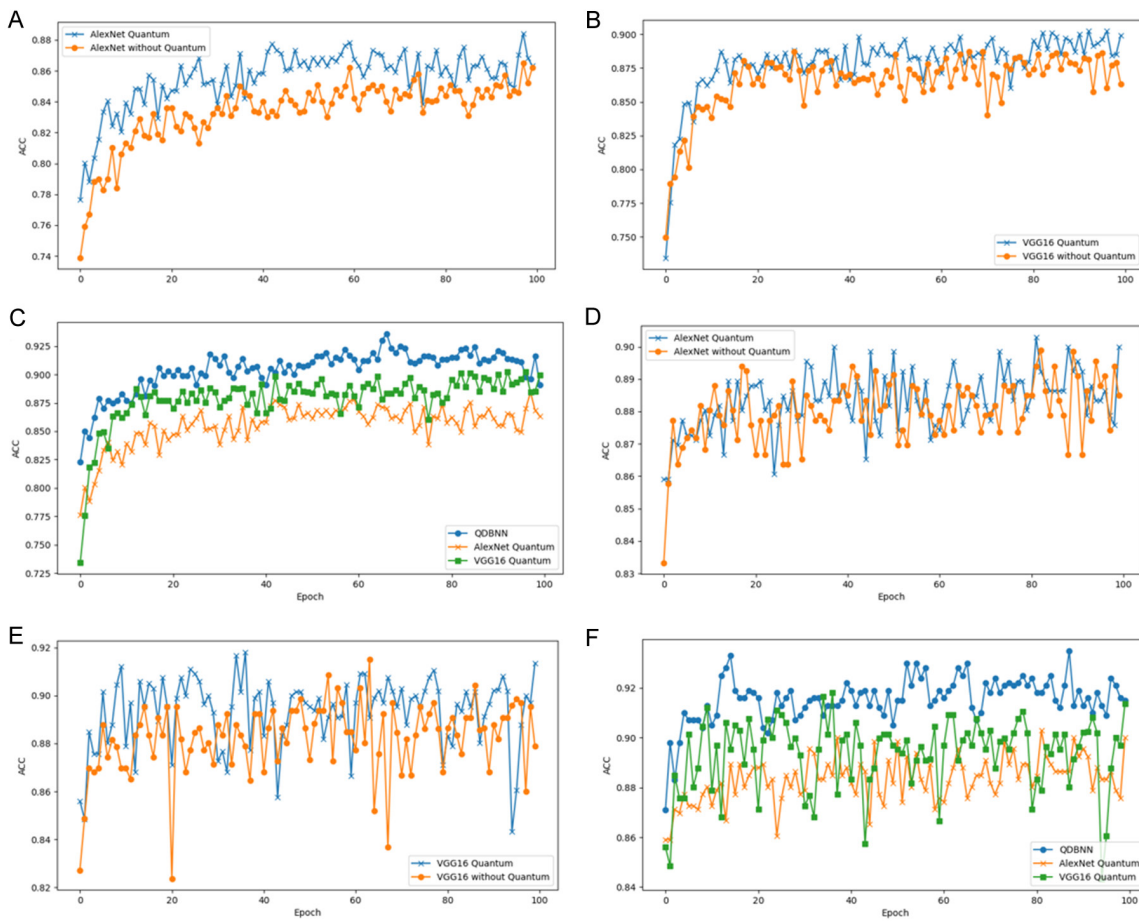


Figure 7. QDBNN comprehensive comparative analysis of AlexNet, VGG16, and QDBNN: accuracy comparisons on HAM10000 and Malignant vs. Benign datasets.

$$F1_{\text{weighted}} = \frac{\sum_{i=1}^n (TP_i + FN_i) \times F1_i}{\sum_{i=1}^n (TP_i + FN_i)}$$

Where TP_i , FN_i , and $F1_i$ are the true positive examples, false negative examples, and $F1$ scores of the i -th category, respectively.

Comprehensive experiments on the HAM10000 dataset compared conventional transfer learning approaches with quantum transfer learning methodologies. As shown in **Figure 7A**, after 100 training rounds, the classic AlexNet model achieved an accuracy of 86.5%, while the AlexNet model using quantum transfer learning reached an accuracy of 88.4%. **Figure 7B** illustrates the performance comparison between classical VGG16 (88.6% accuracy) and its quantum transfer learning variant (90.2% accuracy). Quantum systems offer richer feature representation capabilities, enabling the

extraction of more complex feature relationships. The quantum layer better captures implicit relationships within the data, thereby enhancing classification and recognition accuracy.

In **Figure 7C** illustrates that the QDBNN model attained an initial accuracy of 82.3%, achieved stability after approximately 30 epochs, and ultimately reached 93.6% accuracy. In **Table 1**, when compared to the VGG16 quantum transfer learning model and the AlexNet quantum transfer learning model, QDBNN outperformed all other models, achieving the highest accuracy of 93.6% on dermoscopic images. As a classic multi-class classification problem, traditional quantum methods often show limitations in performance. However, the QDBNN model demonstrated superior performance, highlighting its enhanced generalization ability and robustness.

Table 1. HAM10000 dataset data comparison

Model	Accuray (%)	F1-score (%)
VGG16	88.6	88.4
Alexnet	86.5	85.7
Vgg16_qcnn	90.2	89.4
Alexnet_qcnn	88.4	88.6
Proposed Method	93.6	93.2

Table 2. Skin cancer: Malignant vs. Benign data comparison

Model	Accuray (%)	F1-score (%)
Vgg16	91.5	91.6
Alexnet	89.4	88.8
Vgg16_qcnn	91.8	92.0
Alexnet_qcnn	90.0	89.8
Proposed Method	93.5	93.4

Figure 7D and **7E** present the experimental results where classical transfer learning implementations of AlexNet and VGG16 achieved peak accuracies of 89.4% and 91.5%, respectively. In contrast, the quantum transfer learning versions of AlexNet and VGG16 attained accuracies of 90% and 91.8%. Both the classical and quantum transfer learning methods for VGG16 and AlexNet demonstrated strong performance. However, in **Table 2**, when compared with the HAM10000 dataset, the improvement in performance with quantum networks was not highly significant. Nevertheless, as shown in **Figure 7F**, QDBNN continued to show its advantage, reaching an accuracy of 93.5%. This indicates that QDBNN maintains a clear performance edge over other quantum and classical transfer learning methods. This result confirms that QDBNN effectively integrates features extracted by different networks in skin cancer lesion classification tasks, leading to substantial improvements in both accuracy and F1 score. Therefore, QDBNN proves to be both a rational and effective approach.

Discussion

Table 3 demonstrates our method's superior performance in skin lesion classification on the HAM10000 dataset. The Dempster-Shafer theory [13] ensemble model achieved a maximum accuracy of 92%, while the 1-D multiheaded CNN method [12] only achieved an accuracy of

Table 3. Comparison of QDBNN with recent methods on the Ham10000 dataset

Model	Accuray (%)	F1-score (%)
InceptionResNetV2 [14]	86.00	--
Wide-ShuffleNet [17]	86.33	--
DenseNet-121 [26]	81.00	--
EfficientNET-B1 [18]	84.3	--
1-D multiheaded CNN [12]	89.71	89.12
Dempster-Shafer fusion [13]	92	92
Proposed Method	93.6%	93.2%

Table 4. Comparison of QDBNN with recent methods on the Malignant vs. Benign dataset

Model	Accuray (%)	F1-score (%)
Anup and Vanmathi - AWO [27]	91.9	--
Anup and Vanmathi - DL [27]	90.4	--
Anup and Vanmathi - TL [27]	89.3	--
VGG16 [15]	93.18	--
ResNet152 [28]	89.65	--
Deep-skin [16]	87.8	--
Proposed Method	93.5	93.4

89.71% and an F1 score of 89.12%. While these approaches demonstrate incremental improvements in classification performance, our quantum algorithm-based method for feature extraction and classification exhibited markedly superior results.

Table 4 presents comparative results on the Malignant vs. Benign dataset, where Huang S and Lei H introduced Deep-skin [25], a dermoscopic image classification model integrating attention mechanisms with ensemble learning. Different attention mechanisms were embedded in Inception-V3 to extract potential features, and classification performance was enhanced through late model fusion, achieving a maximum accuracy of 87.8%. Hasan MR [15] reported 93.18% accuracy using the VGG16 network, while our proposed method demonstrated superior performance with 93.5% accuracy.

Our findings demonstrate that QDBNN's dual-branch quantum-classical hybrid architecture achieves robust performance improvements in skin cancer classification. By integrating independently trained quantum-based convolution-

al neural networks branches (AlexNet and VGG16) and fusing their extracted features, the model captures complementary information about lesion morphology, color, and texture. The variational quantum classifier further refines decision boundaries, leveraging the expressive power of quantum layers. Notably, the dual-branch design addresses critical challenges in medical image analysis: it mitigates class imbalance in datasets like HAM10000 by combining feature extraction biases from distinct networks, improves generalization across underrepresented lesion types, and reduces sensitivity to quantum noise inherent in Noisy Intermediate-Scale Quantum (NISQ) devices. The complementary signals between branches offset noise-induced errors in individual pathways, enhancing prediction stability. Additionally, QDBNN demonstrates adaptability across diverse classification scenarios, maintaining consistent performance in both multi-class (HAM10000) and binary (malignant vs. benign) diagnostic tasks.

Despite these advantages, current limitations highlight pathways for future research. Hardware constraints of NISQ devices, including limited qubit counts and gate fidelity, necessitate simulated training environments, though real-device implementation remains a critical goal. The dual-branch architecture's computational complexity, while optimized compared to dual quantum pipelines, still requires resource-intensive training, suggesting potential optimizations through quantum network pruning or lightweight designs. Furthermore, while shallow quantum circuits were employed to avoid gradient vanishing issues, deeper quantum architectures could unlock additional performance gains if coupled with improved noise control in quantum hardware.

These results underscore the potential of quantum-enhanced transfer learning and multi-branch feature fusion in medical imaging. The framework's extensibility to other oncology domains (e.g., breast or lung cancer) and compatibility with advanced techniques like active learning or augmented data pipelines position QDBNN as a promising foundation for clinically robust diagnostic systems. Future progress will depend on co-designing algorithmic innovations with emerging quantum hardware capabilities to bridge the gap between theoretical advantages and practical deployment.

Disclosure of conflict of interest

None.

Address correspondence to: Xing Deng, School of Computer, Jiangsu University of Science and Technology, Zhenjiang 212100, Jiangsu, China. E-mail: xdeng@just.edu.cn

References

- [1] Zhang J, Xie Y, Wu Q and Xia Y. Medical image classification using synergic deep learning. *Med Image Anal* 2019; 54: 10-19.
- [2] Bhattacharya S, Reddy Maddikunta PK, Pham QV, Gadekallu TR, Krishnan S SR, Chowdhary CL, Alazab M and Jalil Piran M. Deep learning and medical image processing for coronavirus (COVID-19) pandemic: a survey. *Sustain Cities Soc* 2021; 65: 102589.
- [3] Yu S, Chen M, Zhang E, Wu J, Yu H, Yang Z, Ma L, Gu X and Lu W. Robustness study of noisy annotation in deep learning based medical image segmentation. *Phys Med Biol* 2020; 65: 175007.
- [4] Linares MA, Zakaria A and Nizran P. Skin cancer. *Prim Care* 2015; 42: 645-659.
- [5] Brinker TJ, Hekler A, Utikal JS, Grabe N, Schadendorf D, Klode J, Berking C, Steeb T, Enk AH and von Kalle C. Skin cancer classification using convolutional neural networks: systematic review. *J Med Internet Res* 2018; 20: e11936.
- [6] Arel I, Rose DC and Karnowski TP. Deep machine learning - a new frontier in artificial intelligence research [Research Frontier]. *IEEE Comput Intell Mag* 2010; 5: 13-18.
- [7] Anguita D, Ridella S, Rivieccio F and Zunino R. Quantum optimization for training support vector machines. *Neural Netw* 2003; 16: 763-770.
- [8] Cong I, Choi S and Lukin MD. Quantum convolutional neural networks. *Nat Phys* 2019; 15: 1273-1278.
- [9] Qu Z, Li Y and Tiwari P. QNMF: a quantum neural network based multimodal fusion system for intelligent diagnosis. *Information Fusion* 2023; 100: 101913.
- [10] Kim J, Huh J and Park DK. Classical-to-quantum convolutional neural network transfer learning. *Neurocomputing* 2023; 555: 126643.
- [11] Gajera HK, Nayak DR and Zaveri MA. A comprehensive analysis of dermoscopy images for melanoma detection via deep CNN features. *Biomed Signal Process Control* 2023; 79: 104186.
- [12] Kumar A, Vishwakarma A, Bajaj V and Mishra S. Novel mixed domain hand-crafted features for skin disease recognition using multiheaded CNN. *IEEE Trans Instrum Meas* 2024; 73.

Early detection of skin cancer

- [13] Dakhli R and Barhoumi W. Disagreement serves an explainable ensemble model based on Dempster–Shafer evidence-fusion for an improved skin lesion classification. *Biomed Signal Process Control* 2024; 98: 106761.
- [14] Nguyen VD, Bui ND and Do HK. Skin lesion classification on imbalanced data using deep learning with soft attention. *Sensors* 2022; 22: 7530.
- [15] Hasan MR, Fatemi MI, Moniruzzaman Khan M, Kaur M and Zagaria A. Comparative analysis of skin cancer (benign vs. malignant) detection using convolutional neural networks. *J Healthc Eng* 2021; 2021: 5895156.
- [16] Huang S, Lei H, Yang J, Hang T, Jin L, Yao Y, Grzegorzek M and Li C. An attention mechanism and ensemble learning based on dermoscopic image classification. *J Imaging Sci Technol* 2024; 68.
- [17] Hoang L, Lee SH, Lee EJ and Kwon KR. Multi-class skin lesion classification using a novel lightweight deep learning framework for smart healthcare. *Applied Sciences* 2022; 12: 2677.
- [18] Tajerian A, Kazemian M, Tajerian M and Akhavan Malayeri A. Design and validation of a new machine-learning-based diagnostic tool for the differentiation of dermatoscopic skin cancer images. *PLoS One* 2023; 18: e0284437.
- [19] Tschandl P, Rosendahl C and Kittler H. The HAM10000 dataset, a large collection of multi-source dermatoscopic images of common pigmented skin lesions. *Sci Data* 2018; 5: 180161.
- [20] Pratt WK, Kane J and Andrews HC. Hadamard transform image coding. *Proceedings of the IEEE* 1969; 57: 58-68.
- [21] Ovalle-Magallanes E, Alvarado-Carrillo DE, Avina-Cervantes JG, Cruz-Aceves I and Ruiz-Pinales J. Quantum angle encoding with learnable rotation applied to quantum-classical convolutional neural networks. *Appl Soft Comput* 2023; 141: 110307.
- [22] Krizhevsky A, Sutskever I and Hinton GE. Imagenet classification with deep convolutional neural networks. *Adv Neural Inf Process Syst* 2012; 25.
- [23] Simonyan K and Zisserman A. Very deep convolutional networks for large-scale image recognition. *arXiv* 2014.
- [24] Mitarai K, Negoro M, Kitagawa M and Fujii K. Quantum circuit learning. *Physical Review A* 2018; 98: 032309.
- [25] Yang J, Yang JY, Zhang D and Lu JF. Feature fusion: parallel strategy vs. serial strategy. *Pattern Recognition* 2003; 36: 1369-1381.
- [26] Gajera HK, Nayak DR and Zaveri MA. A comprehensive analysis of dermoscopy images for melanoma detection via deep CNN features. *Biomed Signal Process Control* 2023; 79: 104186.
- [27] Kumar KA and Vanmathi C. Optimization driven model and segmentation network for skin cancer detection. *Computers & Electrical Engineering* 2022; 103: 108359.
- [28] Hossain M, Sadik K, Rahman MM, Ahmed F, Bhuiyan MNH and Khan MM. Convolutional neural network based skin cancer detection (Malignant vs Benign). *IEEE* 2021; 0141-0147.